Fluidized bed heat exchange capacity of Alumina, coal-char and bio-char solids

F Mushtaq[1], I Ullah[1,2], I Khan[1], S K Sami[1], W Alam[1], M Sadiq[1], Z Tariq[1]and A Jaan[1]

[1]Faculty of Engineering and Architecture, Department of Chemical Engineering, Balochistan University of Information Technology, Engineering and Management Sciences (BUITEMS), Airport Road, Baleli, Quetta, Balochistan, Pakistan.
[2]National Engineering Research, Center of Chemical Fertilizer Catalyst, College of Chemical Engineering, Fuzhou University, Fuzhou, PR China.

Email. faisal.mushtaq@buitms.edu.pk

Abstract. Fluidized bed heat exchanger (FBHx) units have significant applications in various industrial processes. Heat transfer coefficient, pressure drop and superficial gas velocity are the most salient parameters used to characterize the behavior of solid particles in FBHx. This research identifies the pressure drop and surface heat transfer coefficient of Alumina, coal-char and bio-char solids in FBHx. The pressure drop and heat transfer coefficient were estimated at fixed bed height of 6cm by maintaining air flow rate of 8-100 Liters per minute (LPM). Digital temperature sensors are used to measure the bed temperature, air inlet temperature, and heater surface temperature. The results of this study suggest that the effects on pressure drop and surface heat transfer coefficient in FBHx are influenced by bed materials. Among the tested materials, pressure drop and heat transfer coefficient were found of order Alumina>coal-char>bio-char.
Keywords. Fluidized bed heat exchanger, pressure drop, superficial gas velocity, surface heat transfer coefficient, carbon solids.

1. Introduction

Fluidization bed units share the characteristics flow of fluid, where gas or liquid moved through bed of solid particles. A fluid like behavior is attained when the force exerted by the liquid or gas on solid particles in the direction of force and buoyant forces minimizes the downward gravitational forces acting on solid particles. Owning to the corresponding motion, fluidization of the solids can be achieved using gas or liquid phase. Fluidized beds are frequently used as reactors where the gas or liquid is contacted with suspended solids usually used as a catalyst [1-3]. Fluidized bed reactors (FBR) are considered valuable source in industrial applications because they offer high rate of mass transfer and less pressure drop [4]. In addition, FBR presents high rate of mixing and capacity to operate in continuous phase [5]. Fluidized bed heat exchange (FBHx) units offers much complicated heat and mass transport mechanism, where the heat carried by the gas or liquid is used to exchange heat to free flowing solid to raise the solids temperature to desired conditions, and later the reaction carried out at the surface of solids eventually transport mass back [6, 7]. FBHx can be categorized into four classes; i) catalytic gas reactor, where the reactants and products are in the gas phase, and the reaction takes places on the solid surface, either the reactant gases are brought to or solids are pre-heated and maintained to desired temperature ii) reaction gases which utilizes solids as a source of heat energy to

bring the desired reaction conditions, where the reactants and the products are in the gas phase but solids used as heat carrier source iii) gas-solid combination, where the reactants and products are in the gas and solid phase iv) fluidization with no chemical reaction, where the product gases are dried over solid surface [8].

Gas-solids fluidization regimes follows the sequence stationary bed> bubbling bed> slugging bed> turbulent bed >fast moving bed> pneumatic conveying bed, where stationary bed regime refer to minimum fluidization velocity (U_{mf}) that does not tends to move the solid bed. However, with the increase in superficial gas velocity (U_g), the system approaches bubbling bed regime, where the bubbles initiate mixing of solids [8]. U_{mf} is considered as one of the most significant property when describing the fluidization behavior in FBHx [9]. Several methods described in literature are used to estimate U_{mf} in fluidized bed by; i) heat transfer method, ii) pressure drop method and iii) voidage method. In first method, wall heat transfer coefficient is estimated with the increase in gas velocity and the point is noted where heat transfer coefficient increase significantly [8, 10]. This method of finding U_{mf} is quite costly and requires developed experimental setup [11], where heat transfer data are estimated by maintaining steady state conditions. In the second method, pressure drop over the bed and U_g are plotted and point of alteration between stationary and bubbling bed regime are indentified. In third method, U_{mf} is identified when the free space inside the bed begin to increase the bed extension as the U_g increases. Although voidage method is most generally used, however it is difficult to position out the point where bed extension actually begins. In general, U_{mf} mainly depends on physico-chemical properties of solids, liquid and gas phase and bed geometry [10].

Fluidization of bio-char and coal-char solids produced from various industrial applications provides a prospect to develop and utilize by-product carbon rich solids. Several researcher have found widespread applications of bio-char and coal-char as a source of carbon material, such as metallurgical and mineral processing [12], biomass valorization [13], bio-solid handling [14], soil decontamination [15], carbon catalyzed gas-phase reactions [16]. Among these, gas-phase reactions catalyzed over carbon in FBHx are gaining importance over the recent decade [17-20]. The key concerns of using carbon in FBHx are non-uniform nature and variation in density associated with carbons, such as bio-char and coal-char solids which offers complex multiphase system. The effects of significant properties on FBHx capacity needs to be investigated for improved system performance and design. The primary aim of this study is to investigate the effect of air flow rate on pressure drop, U_{mf} and surface heat transfer coefficient of Alumina, bio-char and coal-char solids.

2. Materials and Methods

The coal samples in the form of lumps were collected from the Machh Bolan Mine Company located at Quetta, Pakistan. Sawdust waste biomass samples were collected from local carpenter shop. The coal and sawdust samples of 3 kg were kept in air tight plastic bags and labeled for further processing. The coal and sawdust samples were subjected to combustion at temperature of 550^{o}C and 350^{o}C, respectively for char production. The maximum combustion temperature of coal and sawdust were selected and based on the studies [21, 22]. The coal-char and bio-char samples were sieved to obtain uniform particle of 14 and 20 mesh size, respectively and were used without physico-chemical modification. Granular fused Alumina (white Aluminum Oxide) type V of density 3770 kg/m^3 and 80 grit size (average particle size 177 µm) and pour density of approximately 1620 kg/m^3 was used as a reference material. SOLTEQ® fluidization and fluid bed heat transfer Unit (Model: HE 162) apparatus was used as shown in Figure 1.

The unit comprised of glass cylinder was carefully loaded with 1.25 kg of tested sample and leveled. The glass chamber is coupled with air distributor chamber that supports the bed material at the bottom. The air distributor chamber provided was designed to keep uniform airflow distribution with minimal pressure drop. The air passes through the bed material and vent to atmosphere through an air filter at the top. The bed temperature was measured by thermocouple labeled as T_1. Compressed air was supplied through filter and pressure regulator assembly and airflow rotameters equipped with low flow rate (V) 6-50 liters per minutes (LPM) and high flow 40-440 LPM through air flow control

valves before entering the distribution chamber. The compressed air temperature was measured with thermocouple (T_2). Variable transformer provided with electrical heater power of 250 W and surface area of 22.8 cm^2 was used to control input heater power (Q). The heating element fitted with thermocouple was used to determine the heater surface temperature (labeled as T_3). The pressure drop across the bed at various levels was measured by liquid filled manometer upto 300mm H_2O pressure drop. For excessive pressure in chamber, the chamber is fitted with pressure relief valve.

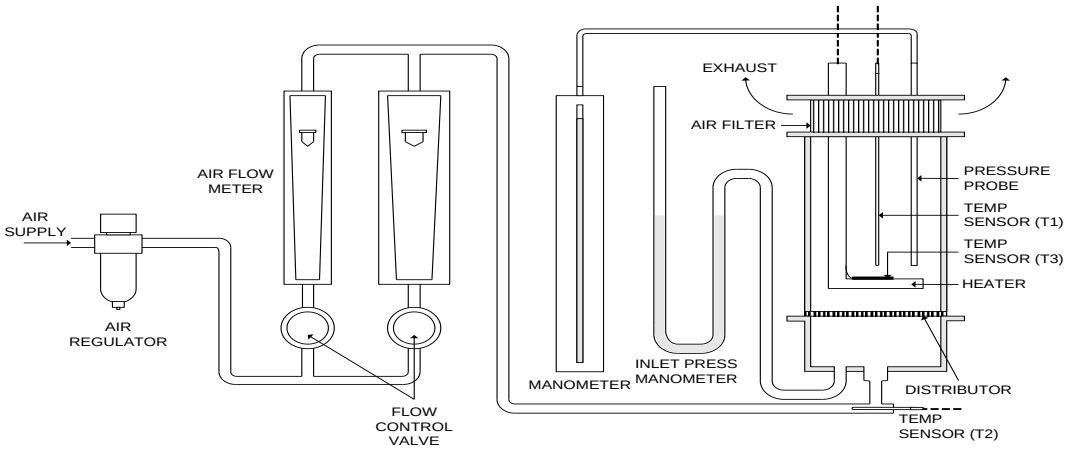

Figure 1. Schematic Diagram of Fluidization and Fluid Bed Heat Exchanger (Model: HE 162) used in this study.

The pressure drop across the bed Δp was measured and is equal to the effective weight of the bed per unit area.

$$\Delta p = M / \rho_p \, Sb \, (\rho_p - \rho_f) \, g \qquad (1)$$

Where mass M of particles of density ρ_p charged in the bed of cross-sectional area Sb fluidized by a fluid of density ρ_f and g gravitational acceleration.

The U_{mf} under ambient conditions was measured by charging 1.25 kg of particles into the chamber to form a bed. Initially, the bed is vigorously fluidized for 1-2 minutes to breakdown particle interlocking. The pressure drop under these conditions was found decreasing as the fluidizing gas velocity was reduced. Several step measurements of the pressure drop across the bed as function of reducing fluidizing gas velocity were noted. The results were plotted as of bed pressure drop and superficial gas velocity. The U_{mf} is derived from the velocity profile, where the intersection between the raising and smoothing of the profile identified. It was expected that the pressure drop tends to have value equal to or less than (because of bed column particle-wall interaction) bed weight per unit area. However, the increase in U_{mf} linearly increases the pressure drop across the bed until the bed approaches fluidization, a condition where gas flow through bed is considered laminar.

The surface heat transfer coefficient is calculated using Equation 2.

$$h = Q / A_h \, \Delta T_m \qquad (2)$$

Where Q is the heater power in W in $W/m^2.K$, A_h is surface area of the heater in m^2 and ΔT_m is the mean temperature difference in K and calculated from

$$\Delta T_m = \Delta T_1 - \Delta T_2 \qquad (3)$$

Where ΔT_1 is the temperature difference between heater surface (T_3) and air inlet (T_2) and ΔT_2 is the temperature difference between heater surface (T_3) and bed material (T_1).

The following are the details of calculations:

For superficial gas velocity

a. Material= Al_2O_3, mean particle diameter=d_p=177 μm (80grit), particle density= ρ_p=3770kg/m^3, mass of the particles=m=1.25kg, Air flow through bed, V_b= (V/60)x(T_1/T_2) and superficial gas velocity , U_g=V_b/(1000 x A), where, cross sectional area of the bed= A= 0.008659 m^2

b. Material= Coal-char, mean particle diameter=d_p=1410 μm (14 mesh), particle density= ρ_p=0.0009kg/m^3, mass of the particles=m=1.25kg, Air flow through bed, V_b= (V/60)x(T_1/T_2) and superficial gas velocity , U_g=V_b/(1000 x A), where, cross sectional area of the bed= A= 0.008659 m^2

For surface heat transfer coefficient

a. Material= Al_2O_3, mean particle diameter=d_p=177μm (80grit), particle density= ρ_p=3770kg/m^3, mass of the particles=m=1.25kg, Air flow through bed, V_b= (V/60)x(T_1/T_2) and superficial gas velocity , U_g=V_b/(1000 x A), where cross sectional area of the bed= A= 0.008659 m^2, surface heat transfer coefficient=h= Q/A_h x ΔT_m, ΔT_m=ΔT_1 – ΔT_2 (where ΔT_1= T_3 – T_2 and ΔT_2= T_3 – T_1) and A_h= surface heat transfer area of heater= 0.00228 m^2

b. Material= Coal-char, mean particle diameter=d_p=1410 μm (14 mesh), particle density= ρ_p=0.0009kg/m^3, mass of the particles=m=1.25kg, Air flow through bed, V_b= (V/60)x(T_1/T_2) and superficial gas velocity , U_g=V_b/(1000 x A), where cross sectional area of the bed= A= 0.008659 m^2, Surface heat transfer coefficient=h= Q/A_h x ΔT_m, ΔT_m=ΔT_1 – ΔT_2 (where ΔT_1= T_3 – T_2 and ΔT_2= T_3 – T_1) and A_h= surface heat transfer area of heater= 0.00228 m^2

c. Material= Bio-char, mean particle diameter=d_p=841 μm (20 mesh), particle density= ρ_p=0.0003 kg/m^3, mass of the particles=m=1.25kg, Air flow through bed, V_b= (V/60)x(T_1/T_2) and superficial gas velocity , U_g=V_b/(1000 x A), where cross sectional area of the bed= A= 0.008659 m^2, Surface heat transfer coefficient=h= Q/A_h x ΔT_m, ΔT_m=ΔT_1 – ΔT_2 (where ΔT_1= T_3 – T_2 and ΔT_2= T_3 – T_1) and A_h= surface heat transfer area of heater= 0.00228 m^2

3. Results and Discussion

3.1. Effects of change in bed height, bed pressure drop and upward air flow velocity of Al_2O_3 granular bed

The results of change in bed height, pressure drop with increasing and decreasing air flow rate is given in Table 1 and Table 2 and redrawn as Figure 2 and Figure 3 as a function of superficial gas velocity, bed height and pressure drop. As can be observed from Table 1 and 2 that pressure drop is directly proportional to the superficial gas velocity. At low air flow rate, drastic increase in pressure drop can be related to lesser penetration of air within the bed material. However, pressure drop was observed fairly constant during later stages of fluidization. This is mainly due to the fact that particles are kept separated ensuing higher free space and increase in viodage. The U_{mf} calculated of 0.04 m/s at 97 mm of H_2O/mm of bed height from Figure 3.

Table 1. Effects bed height, pressure drop and air flow velocity of Al_2O_3 bed with increasing air flow rate.

Air flow rate (*LPM*)	T_1(*K*)	T_2(*K*)	H (*mm*)	V_b *(L/s)*	U_g (*m/s*)	Δ*P/bed height* (*mm of H_2O/mm*)
8	307.5	306.5	60	0.13	0.015	55.3
12	309.3	306.5	61	0.20	0.023	76.4
16	309.1	306.4	69	0.27	0.031	102.8
20	309.6	306.5	73	0.34	0.039	124.7
24	311.6	306.5	81	0.41	0.047	96.6
30	313.9	306.4	85	0.51	0.059	97.4
40	310.7	307.6	89	0.67	0.078	99.7
60	310.4	306.6	93	1.01	0.117	101.6
80	311.2	306.7	97	1.35	0.156	104.8
100	311.3	307	115	1.69	0.195	108.6

Table 2. Effects of bed height, pressure drop and air flow velocity of Al_2O_3 bed with decreasing air flow rate.

Air flow rate (*LPM*)	$T_1(K)$	$T_2(K)$	H (*mm*)	V_b *(L/s)*	U_g (*m/s*)	*ΔP/bed height (mm of H_2O/mm)*
100	316.6	299.5	80	1.76	0.20	111.4
80	315.4	299.2	73	1.41	0.16	106.6
60	315.9	298.6	70	1.06	0.12	103.8
40	306.5	298.1	68	0.69	0.08	101.2
30	304.2	297.8	65	0.51	0.06	100.5
24	296.9	297.3	62	0.40	0.05	99.8
20	296.3	296.9	60	0.33	0.04	95.2
16	296.1	296.2	59	0.27	0.03	80.2
12	295.9	295.7	59	0.20	0.02	58.5
8	295.4	295.4	59	0.13	0.02	41.8

3.2. Effects of change in bed height, bed pressure drop and upward air flow velocity of coal-char bed

The results of change in bed height, pressure drop with increasing and decreasing air flow rate is given in Table 3 and 4 and redrawn as Figure 4 and Figure 5 as a function of superficial gas velocity, bed height and pressure drop. As can be observed from Table 3 and 4, pressure drop increases with increase in superficial gas velocity at low to moderate air flow rate, which can be related to lesser penetration of air within the compacted bed material. However, once the bed is fluidized, pressure drop was observed fairly constant. The U_{mf} determined was equal to 0.116 m/s from Figure 5. The maximum pressure drop with coal-char bed was observed 33.12 mm of H_2O/mm of bed height, where Al_2O_3 bed of the same mass produced 111.4 mm of H_2O/mm of bed height. U_{mf} was estimated at 0.116 m/s at 21.5 mm of H_2O/mm of bed height pressure drop. This difference can be correlated to large difference is density.

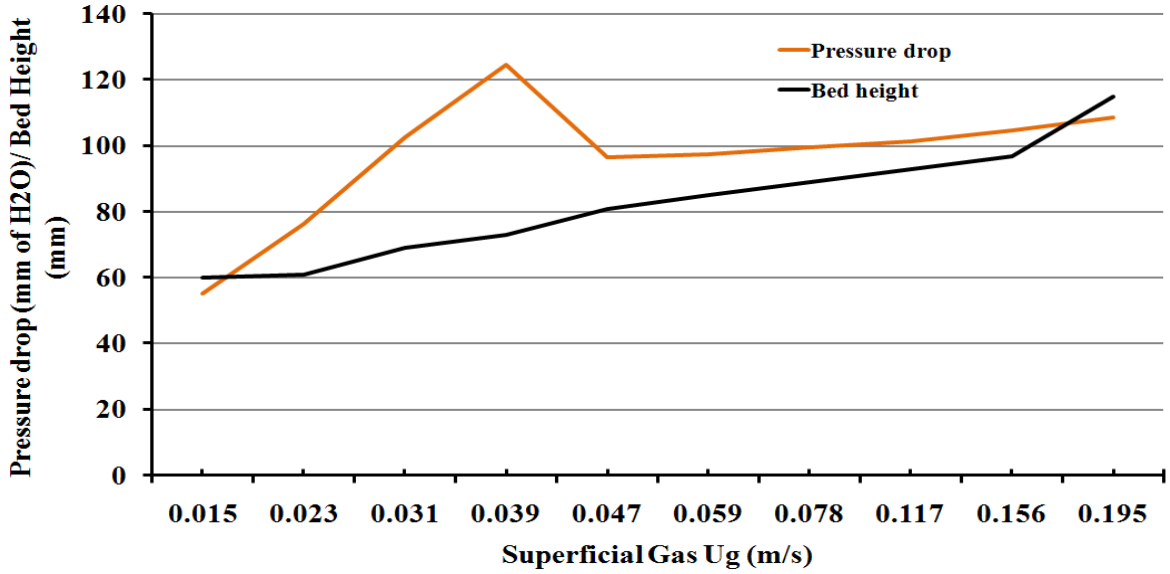

Figure 2. Effects of superficial gas flow on pressure drop and bed height of Al_2O_3 with increasing air flow rate

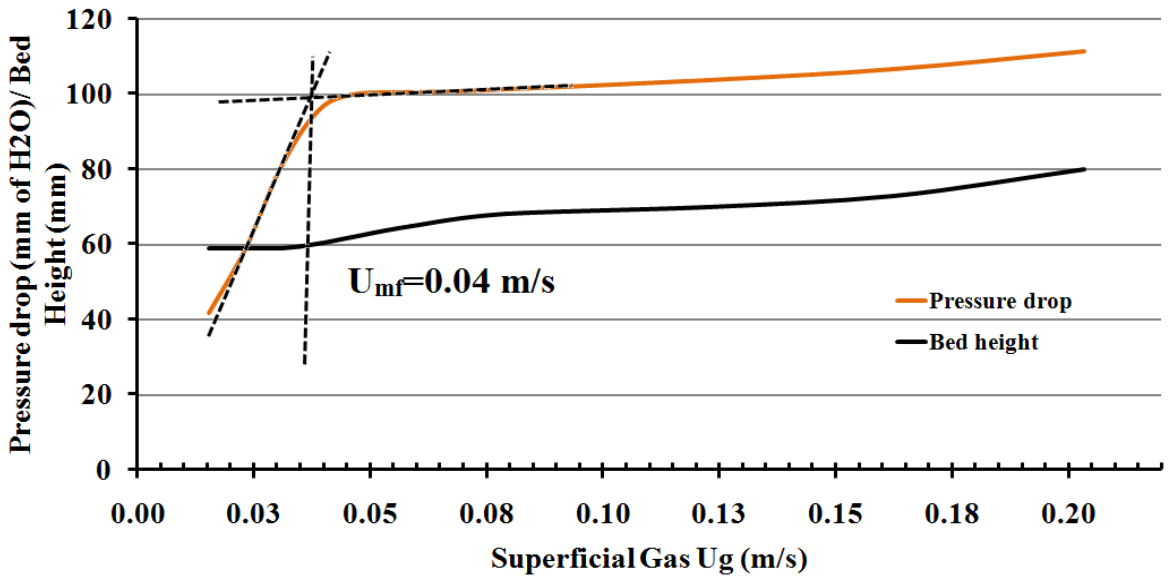

Figure 3. Effects of superficial gas flow on pressure drop and bed height of Al_2O_3 with decreasing air flow rate

Table 3. Effects of change in bed height, pressure drop of coal-char bed with increasing air flow rate.

Air flow rate (*LPM*)	$T_1(K)$	$T_2(K)$	H (*mm*)	V_b *(L/s)*	U_g (*m/s*)	Δ*P/bed height* (*mm of H_2O/mm*)
8	307.5	306.5	60	0.13	0.015	7.62
12	309.3	306.5	61	0.20	0.023	25.4
16	309.1	306.4	69	0.26	0.031	32.02
20	309.6	306.5	73	0.33	0.038	30.48
24	311.6	306.5	81	0.39	0.045	31.00
30	313.9	306.4	85	0.49	0.056	38.1
40	310.7	307.6	89	0.66	0.076	33.12
60	310.4	306.6	93	0.99	0.114	33.02
80	311.2	306.7	97	1.31	0.152	22.94
100	311.3	307	115	1.64	0.190	27.94

Table 4. Effects of change in bed height, pressure drop of coal-char bed with decreasing air flow rate.

Air flow rate (*LPM*)	$T_1(K)$	$T_2(K)$	H (*mm*)	V_b *(L/s)*	U_g (*m/s*)	Δ*P/bed height* (*mm of H_2O/mm*)
100	311.3	307	115	1.89019	0.218	27.94
80	311.2	306.7	100	1.64257	0.190	22.94
60	311.2	306.6	93	1.52709	0.176	33.02
40	310.7	307.6	87	1.43553	0.166	33.12
30	313.9	306.4	84	1.36655	0.158	38.1
24	311.6	306.5	81	1.3279	0.153	25.86
20	309.6	306.5	73	1.20448	0.139	30.48
16	309.1	306.4	70	1.15648	0.134	32.02
12	309.3	306.5	62	1.02398	0.118	25.4
8	307.5	306.5	60	0.99675	0.115	7.62

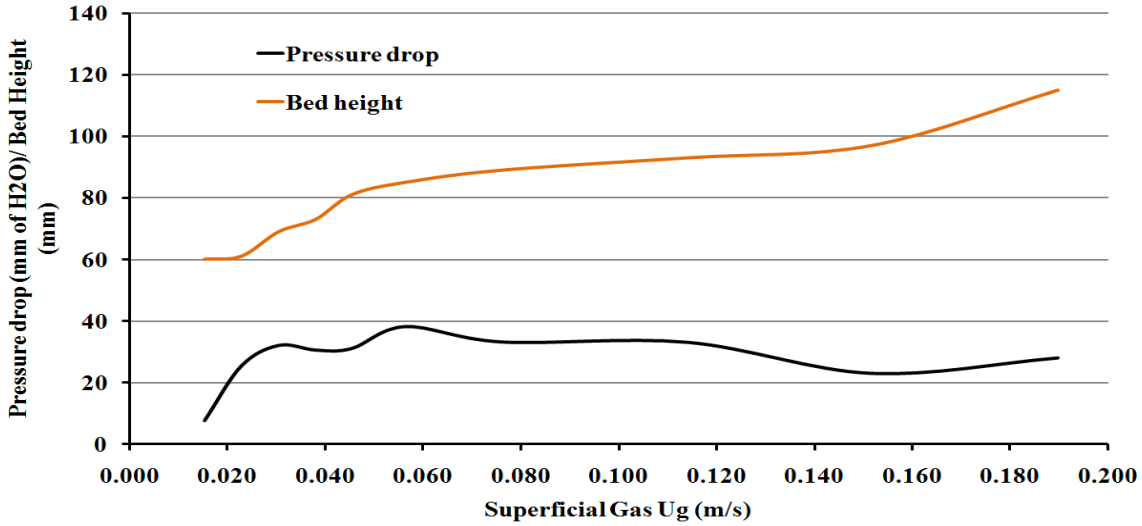

Figure 4. Effects of superficial gas velocity bed height and pressure drop of coal-char with increasing air flow rate

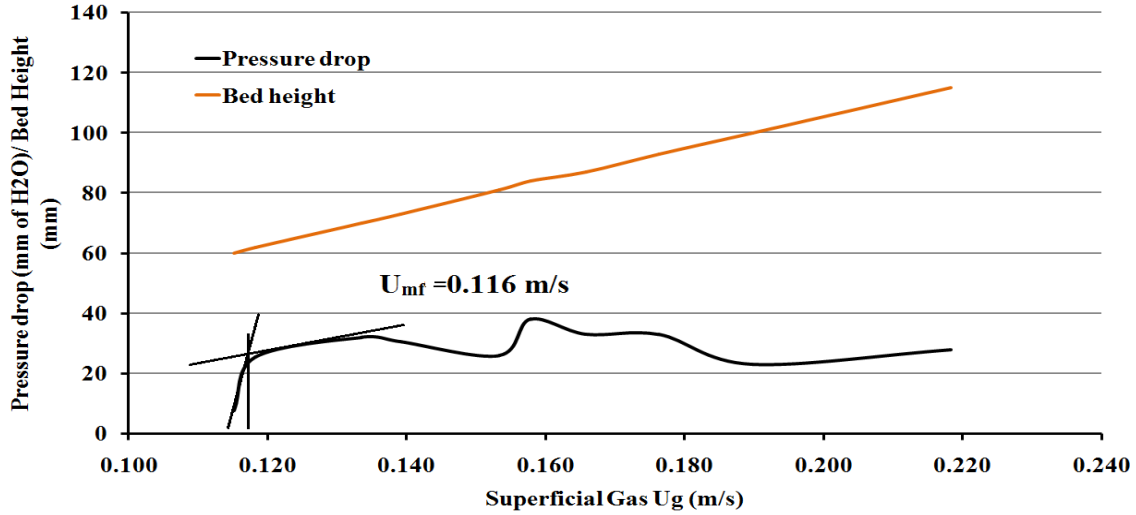

Figure 5. Effects of superficial gas velocity bed height and pressure drop of coal-char with decreasing air flow rate

3.3. Effects of heater power, superficial gas velocity on surface heat transfer coefficient of Al_2O_3, coal-char and bio-char bed

The results of change in heater power and superficial gas velocity on surface heat transfer coefficient of Al2O3, coal-char and bio-char are presented in Table 5, Table 6 and Table 7, respectively and compared in Figure 6. It can be observed that increase in heater power and superficial gas velocity increases the surface heat transfer coefficient with all the tested material. The highest *h* was observed with Al_2O_3 of 717.70 W/m^2.K and lowest with bio-char of 43.76 W/m^2.K. Among the tested material, the surface heat transfer coefficient were observed of order Al_2O_3 >coal-char>bio-char. This difference can be mainly correlated to the difference is physico-chemical properties of the material. The heat exchange capacity in fluidized system of metals and carbon based material can be influenced greatly where the bed is fluidized.

Table 5. Effects of heater power and superficial gas velocity on surface heat transfer coefficient of Al_2O_3

Height of heater (mm)	Height of T_1 Probe (mm)	Air flow rate (LPM)	T_1(K)	T_2(K)	T_3(K)	Heater power Q (W)	V_b (L/s)	Superficial gas Velocity U_g (m/s)	ΔT_m	Surface heat transfer coefficient h (W/m^2.K)
40	40	8	326.4	307.3	356.2	**4.3**	0.142	**0.016**	19.100	98.74
40	40	12	325.7	307.1	356.4	**4.6**	0.212	**0.024**	18.600	108.47
40	40	16	324.4	306.3	356.2	**4.9**	0.282	**0.033**	18.100	118.74
40	40	20	323.2	306.5	356.7	**5.5**	0.351	**0.041**	16.700	144.45
40	40	26	323	307	356.8	**5.7**	0.456	**0.053**	16.000	156.25
40	40	30	321.6	306.4	357	**6.3**	0.525	**0.061**	15.200	181.79
40	40	40	318.3	306.3	356.9	**7.5**	0.693	**0.080**	12.000	274.12
40	40	60	316.5	306.5	357	**9.2**	1.033	**0.119**	10.000	403.51
40	40	80	316.7	306.4	358.5	**11.6**	1.378	**0.159**	10.300	493.95
40	40	100	314.2	306.5	358.3	**12.6**	1.709	**0.197**	7.700	717.70

Table 6. Effects of heater power and superficial gas velocity on surface heat transfer coefficient of coal-char

Height of heater (mm)	Height of T_1 Probe (mm)	Air flow rate (LPM)	T_1(K)	T_2(K)	T_3(K)	Heater power Q (W)	V_b (L/s)	Superficial gas Velocity U_g (m/s)	ΔT_m	Surface heat transfer coefficient h (W/m^2.K)
40	40	8	340.9	305.5	329.8	**4.3**	0.149	**0.017**	35.4	53.28
40	40	12	339.6	305.3	330	**4.6**	0.222	**0.026**	34.3	58.82
40	40	16	338.2	304.5	329.8	**4.9**	0.296	**0.034**	33.7	63.77
40	40	20	338	304.7	330.3	**5.5**	0.370	**0.043**	33.3	72.44
40	40	26	337.8	305.2	330.4	**5.7**	0.480	**0.055**	32.6	76.69
40	40	30	335.4	304.6	330.6	**6.3**	0.551	**0.064**	30.8	89.71
40	40	40	334.1	304.5	329.5	**7.5**	0.731	**0.084**	29.6	111.13
40	40	60	331.3	304.7	330.6	**9.2**	1.087	**0.126**	26.6	151.70
40	40	80	330.5	304.6	334.1	**11.6**	1.447	**0.167**	25.9	196.44
40	40	100	330	306.7	333.9	**12.6**	1.793	**0.207**	23.3	237.18

Table 7. Effects of heater power and superficial gas velocity on surface heat transfer coefficient of bio-char

Height of heater (mm)	Height of T_1 Probe (mm)	Air flow rate (LPM)	T_1(K)	T_2(K)	T_3(K)	Heater power Q (W)	V_b (L/s)	Superficial gas Velocity U_g (m/s)	ΔT_m	Surface heat transfer coefficient h (W/m^2.K)
40	40	8	340.9	305.5	329.8	**4.3**	0.149	**0.017**	35.4	53.28
40	40	12	339.6	305.3	330	**4.6**	0.222	**0.026**	34.3	58.82
40	40	16	338.2	304.5	329.8	**4.9**	0.296	**0.034**	33.7	63.77
40	40	20	338	304.7	330.3	**5.5**	0.370	**0.043**	33.3	72.44
40	40	26	337.8	305.2	330.4	**5.7**	0.480	**0.055**	32.6	76.69
40	40	30	335.4	304.6	330.6	**6.3**	0.551	**0.064**	30.8	89.71
40	40	40	334.1	304.5	329.5	**7.5**	0.731	**0.084**	29.6	111.13
40	40	60	331.3	304.7	330.6	**9.2**	1.087	**0.126**	26.6	151.70
40	40	80	330.5	304.6	334.1	**11.6**	1.447	**0.167**	25.9	196.44
40	40	100	330	306.7	333.9	**12.6**	1.793	**0.207**	23.3	237.18

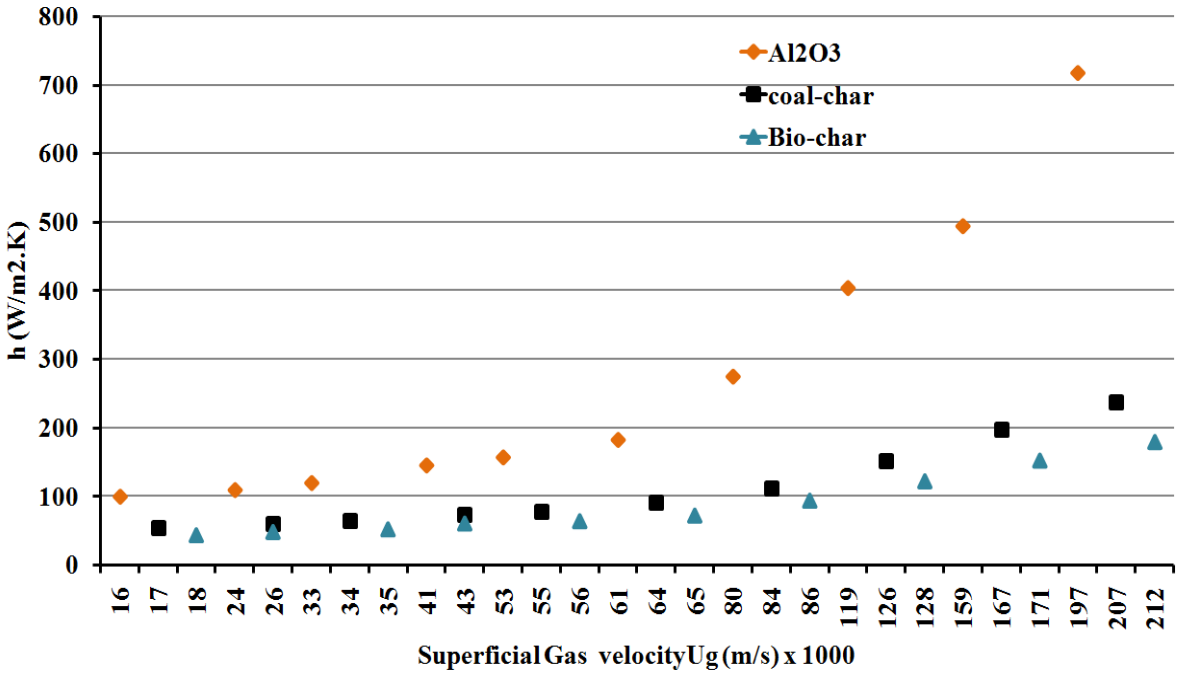

Figure 6. Comparison of surface heat transfer coefficient of the tested material

4. Conclusion

This study investigated the effects of change in bed height, bed pressure drop and upward air flow velocity on superficial gas velocity and fluidization behavior. Further, the effect of superficial gas velocity on surface heat transfer coefficient of Alumina, coal-char and bio-char were tested. The results of this study suggests that pressure drop increases with increase in superficial gas velocity at low to moderate air flow rate, which can be correlated to lesser penetration of air within the compacted bed material. However, once the bed is fluidized, pressure drop was observed fairly constant which is mainly due to the increase in free viodage space. In addition, increase in heater power and superficial gas velocity increases the surface heat transfer coefficient with all the tested material. Among the material tested, the surface heat transfer coefficient were observed of order Al_2O_3 >coal-char>bio-char. The intermediate heat exchange properties of coal-char suggests potential application as slow raise in bed solid temperature and controls over final process temperature when tested as catalyst in bench scale fluidized bed reactor.

Acknowledgement

Authors gratefully acknowledge the support of Balochistan University of Information Technology, Engineering and Management Sciences (BUITEMS), Quetta, Balochistan, Pakistan.

References

[1] Aho A, Kumar N, Eränen K, Salmi T, Hupa M and Murzin D Y 2007 Catalytic pyrolysis of biomass in a fluidized bed reactor: influence of the acidity of H-beta zeolite *Process Safety and Environmental Protection* **85** 473-80

[2] Asadullah M, Ito S-i, Kunimori K, Yamada M and Tomishige K 2002 Biomass gasification to hydrogen and syngas at low temperature: novel catalytic system using fluidized-bed reactor *Journal of Catalysis* **208** 255-9

[3] Zhang H, Xiao R, Huang H and Xiao G 2009 Comparison of non-catalytic and catalytic fast pyrolysis of corncob in a fluidized bed reactor *Bioresource Technology* **100** 1428-34

[4] Karmakar M K, Loha C, De S and Chatterjee P K 2018 *Coal and Biomass Gasification*: Springer) pp 93-114
[5] Natarajan E, Nordin A and Rao A 1998 Overview of combustion and gasification of rice husk in fluidized bed reactors *Biomass and bioenergy* **14** 533-46
[6] Kim S D and Kang Y 1997 Heat and mass transfer in three-phase fluidized-bed reactors—an overview *Chemical Engineering Science* **52** 3639-60
[7] Behjat Y, Shahhosseini S and Hashemabadi S H 2008 CFD modeling of hydrodynamic and heat transfer in fluidized bed reactors *International Communications in Heat and Mass Transfer* **35** 357-68
[8] Kunii D and Levenspiel O 2013 *Fluidization engineering*: Elsevier
[9] Molerus O and Wirth K-E 2012 *Heat transfer in fluidized beds* vol 11: Springer Science & Business Media
[10] Wen C and Yu Y 1966 A generalized method for predicting the minimum fluidization velocity *AIChE Journal* **12** 610-2
[11] Gupta C K and Sathiyamoorthy D 1998 *Fluid bed technology in materials processing*: CRC press
[12] Ma Z, Bai J, Li W, Bai Z and Kong L 2013 Mineral transformation in char and its effect on coal char gasification reactivity at high temperatures, Part 1: Mineral transformation in char *Energy & Fuels* **27** 4545-54
[13] Trivedi N S, Mandavgane S A and Chaurasia A 2018 Characterization and valorization of biomass char: a comparison with biomass ash *Environmental Science and Pollution Research* **25** 3458-67
[14] Pang S 2016 *Fuel Flexible Energy Generation*: Elsevier pp 241-69
[15] Menéndez J, Arenillas A, Fidalgo B, Fernández Y, Zubizarreta L, Calvo E G and Bermúdez J M 2010 Microwave heating processes involving carbon materials *Fuel Processing Technology* **91** 1-8
[16] Ma Z, Bai J, Bai Z, Kong L, Guo Z, Yan J and Li W 2014 Mineral transformation in char and its effect on coal char gasification reactivity at high temperatures, part 2: char gasification *Energy & Fuels* **28** 1846-53
[17] Sun L, Luo K and Fan J 2018 Production of synthetic natural gas by CO methanation over Ni/Al2O3 catalyst in fluidized bed reactor *Catalysis Communications* **105** 37-42
[18] Carnevali D, Guévremont O, RIgamonti M G, Stucchi M, Cavani F and Patience G S 2018 Gas-phase fructose conversion to furfural in micro-fluidized bed reactor *ACS Sustainable Chemistry & Engineering* **6** 5580-7
[19] Mattisson T, Keller M, Linderholm C, Moldenhauer P, Rydén M, Leion H and Lyngfelt A 2018 Chemical-looping technologies using circulating fluidized bed systems: Status of development *Fuel Processing Technology* **172** 1-12
[20] Zhu Y, Chen K, Yi C, Mitra S and Barat R 2018 Dry reforming of methane over palladium–platinum on carbon nanotube catalyst *Chemical Engineering Communications* **7** 1-9
[21] Aqsha A, Mahinpey N, Mani T, Salak F and Murugan P 2011 Study of sawdust pyrolysis and its devolatilisation kinetics *The Canadian Journal of Chemical Engineering* **89** 1451-7
[22] Mushtaq F, Qadeer A, Mir F and Aftab A 2012 Coal fired power generation potential of Balochistan *Petroleum & Coal* **54** 132-42